ArtiBench and ArtiBrain: Benchmarking Generalizable Vision-Language Articulated Object Manipulation

Yuhan Wu^{1,*} Tiantian Wei^{2,*} Shuo Wang¹ ZhiChao Wang¹
Yanyong Zhang¹ Daniel Cremers² Yan Xia^{1,†}

¹University of Science and Technology of China

²Technical University of Munich

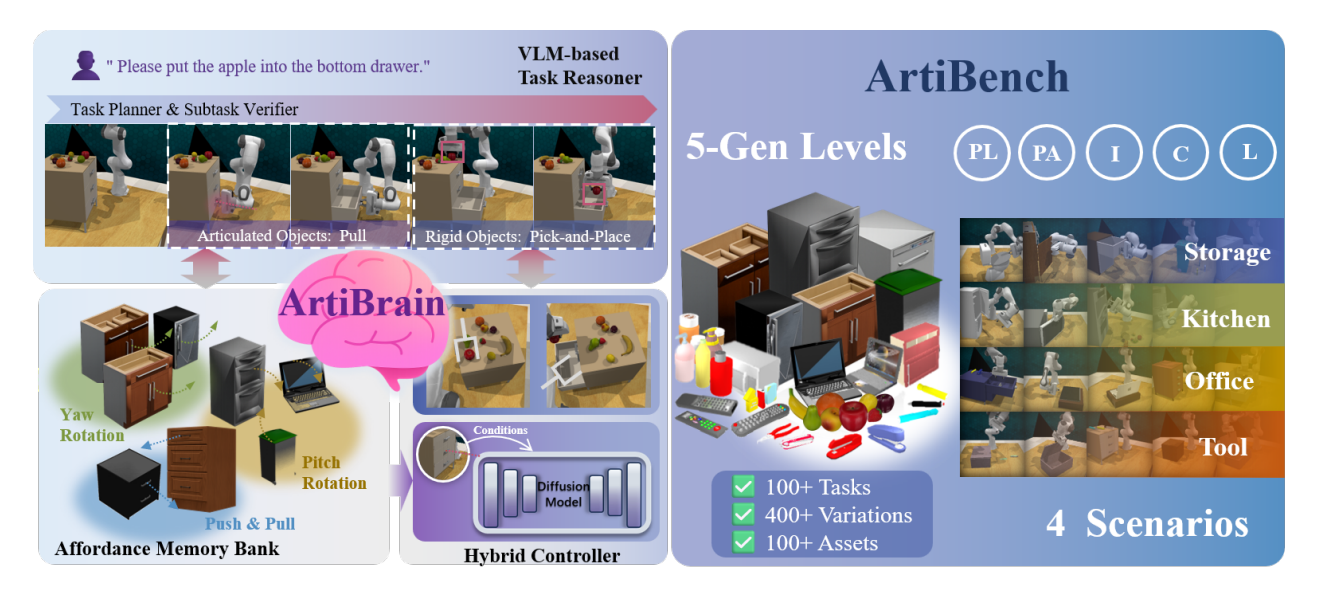


Figure 1. Overview of ArtiBrain and ArtiBench. (*Left*) ArtiBrain performs long-horizon articulated manipulation via hierarchical reasoning and hybrid control. It is a hierarchical, closed-loop framework that integrates three key modules: a VLM-based Task Reasoner, a Hybrid Controller for both rigid and articulated actions, and an Affordance Memory Bank that accumulates verified part-level affordances to enhance transfer across parts and categories. (*Right*) ArtiBench provides 100+ articulated tasks and 400+ variations across four household scenarios and five generalization levels, enabling systematic evaluation from part-level variation to long-horizon multi-object manipulation.

Abstract

Interactive articulated manipulation requires long-horizon, multi-step interactions with appliances while maintaining physical consistency. Existing vision-language and diffusion-based policies struggle to generalize across parts, instances, and categories. We first introduce ArtiBench, a five-level benchmark covering kitchen, storage, office, and tool environments. ArtiBench enables structured evaluation from cross-part and cross-instance variation to long-horizon multi-object tasks, revealing the core generalization challenges of articulated object manipulation. Building on this benchmark, we propose ArtiBrain, a modu-

lar framework that unifies high-level reasoning with adaptive low-level control. ArtiBrain uses a VLM-based Task Reasoner (GPT-4.1) to decompose and validate subgoals, and employs a Hybrid Controller that combines geometry-aware keyframe execution with affordance-guided diffusion for precise and interpretable manipulation. An Affordance Memory Bank continually accumulates successful execution episodes and propagates part-level actionable affordances to unseen articulated parts and configurations. Extensive experiments on ArtiBench show that our ArtiBrain significantly outperforms state-of-the-art multimodal and diffusion-based methods in robustness and generalization. Code and dataset will be released upon acceptance.

^{*}Equal contributions.

[†]Corresponding author.

1. Introduction

Recent advances in robot learning have enabled robots to grasp, place, and rearrange rigid objects in controlled environments [1, 11, 15, 16, 18, 25, 27]. However, real-world tasks often require sequential interactions with articulated objects such as drawers, cabinets, and appliances. These tasks demand more than goal understanding. They require reasoning about articulation states, contact dynamics, and feasible action sequences. For instance, the instruction "clean the desk" involves opening a drawer, retrieving an item, and placing it back. Each step depends on grounding object states and maintaining physical consistency.

Despite progress in robot learning, a gap remains between controlled demonstrations and general embodied intelligence. To act autonomously in diverse articulated environments, robots must interpret open-ended language instructions, decompose them into sub-tasks, and execute them reliably. Recent work has improved language-conditioned planning [6, 13, 21, 22, 31, 32, 57] and affordance-driven control [47, 54]. However, most methods remain limited to rigid-object manipulation or single-step articulated actions [4, 5, 9, 12, 24, 26, 36, 42, 51, 54, 57]. Existing datasets [11, 17, 23, 27, 30, 34, 35, 45, 48] rarely evaluate cross-part, cross-instance, or cross-category generalization. As a result, there is still no unified framework that connects high-level reasoning with reliable low-level execution in articulated environments.

To address this gap, we introduce ArtiBench, a benchmark for articulated-object manipulation. It contains 132 articulated scenes and 449 task variations across four household domains. It defines five generalization levels covering random placement, cross-part, cross-instance, crosscategory, and long-horizon composition, enabling systematic evaluation beyond single-step drawer-opening tasks. Furthermore, we observe that long-horizon articulated tasks couple articulated interactions with rigid-object manipulation, such as picking an item and placing it into a drawer. Rigid-motion phases exhibit predictable geometry and can be efficiently handled through structured keyframe or motion-planning strategies, whereas articulated interactions demand adaptive, contact-aware control. Diffusionbased visuomotor policies excel at capturing contact dynamics but require large-scale expert demonstrations and suffer from sampling latency [46]. In contrast, keyframebased control offers compact policy representations that generalize well in structured motion regimes [2, 49].

Motivated by these observations, we propose ArtiBrain, a hierarchical policy that unifies high-level reasoning and adaptive low-level control for articulated-object manipulation. Inspired by the compositional structure of everyday tasks, we design a VLM-based Task Reasoner that parses natural-language instructions and verifies the scene state to produce structured subgoals with explicit suc-

cess conditions. To execute these subgoals, we introduce a Hybrid Controller that dynamically switches between two control modes: a geometry-guided keyframe policy (GeoKeyframe) for structured rigid-motion phases, and an affordance-guided diffusion policy for contact-rich articulated interactions (ArtiDiffusion). Furthermore, we observe that articulated parts can share transferable affordance priors across categories. To leverage this finding, we develop an Affordance Memory Bank that stores and updates partlevel priors from successful episodes, enabling robust generalization to unseen objects.

To summarize, the main contributions of this work are:

- We address the underexplored problem of long-horizon articulated object manipulation, where robots must jointly reason about part states, contact dynamics, and sequential actions under open-vocabulary instructions.
- We introduce ArtiBench, a comprehensive benchmark with 132 articulated scenes and 449 task variations across four household domains. It defines five generalization levels: random placement, cross-part, cross-instance, cross-category, and long-horizon composition, enabling systematic evaluation beyond single-step actions.
- We propose ArtiBrain, a hierarchical framework that unifies high-level reasoning and low-level control. It comprises a VLM-based Task Reasoner for structured subgoal generation and a Hybrid Controller that integrates two carefully designed policies and an Affordance Memory Bank that enables continual refinement of transferable part-level priors.
- We show that ArtiBrain achieves strong part-level generalization on the proposed ArtiBench, outperforming 3D-LOTUS++ [15] by 67% on novel-part manipulation. It further achieves the best performance on long-horizon articulated tasks among the evaluated baselines, demonstrating consistent generalization from short single-step interactions to complex multi-step manipulation.

2. Related Work

Foundation Models for Task Reasoning and Planning. Large Language Models (LLMs) and Vision Language Models (VLMs) enable high-level reasoning, task decomposition, and open-vocabulary planning in robotics [6, 20, 40, 41, 50, 53]. Prior efforts ground outputs from LLMs or VLMs to executable actions via feasibility value functions [6], language-to-skill translation [20, 40], or multimodal closed-loop prompting [41, 50, 53]. However, they still reason mostly at the semantic level and lack explicit knowledge on how to contact and how to move after contact, resulting in unreliable behavior in contact-rich and multipart manipulation settings. In this work, we bridge this gap by coupling VLM reasoning with articulation-aware control and part-aware affordance transfer mechanism, enabling high-level plans to produce physically feasible action

trajectories.

Diffusion Policies for Visuomotor Control. Diffusion-based visuomotor policies generate actions through conditional denoising. They have shown strong stability and support multimodal action reasoning [9, 19, 36]. Recent 3D extensions incorporate point clouds and multi-view features to enhance spatial grounding [26, 51]. Affordance-conditioned variants further inject contact priors to improve contact precision [47, 54]. However, most diffusion policies are still short-horizon and lack hierarchical structure, making it difficult to generalize across articulated parts and diverse tasks. In this work, we combine VLM-guided hierarchical planning with an articulation-aware diffusion controller to achieve scalable and transferable manipulation in complex articulated environments.

Articulated Object Manipulation Benchmarks. Standardized benchmarks have driven progress in generalizable manipulation, with simulators such as *RLBench* [23], CALVIN [34], ManiSkill [35], iGibson2.0 [29], and AI2-THOR [28] enabling reproducible and scalable evaluation of robotic policies. GEMBench [15], introduces graded generalization splits across instances and categories to assess policy robustness. However, existing benchmarks vary significantly in terms of physics fidelity and generalization scope. RLBench [23] focuses on rigid-object manipulation without articulation reasoning, while VLMBench [55] extends it with vision-language grounding but remains limited in scale and articulation coverage. CALVIN [34] introduces long-horizon reasoning yet contains few assets and limited task diversity. Colosseum [38] targets robustness to environmental variations such as lighting and viewpoint changes rather than generalization across manipulable objects. Although GEMBench [15] expands toward unseen objects and novel tasks, it still lacks systematic part-level and articulation-oriented variations. Our ArtiBench is the first comprehensive benchmark for articulated-object manipulation, offering over 400 unique, systematic part-level and articulation-oriented variations across drawers, cabinets, appliances, and tools.

3. ArtiBench

Our ArtiBench systematically evaluates the generalization capability of articulated-object manipulation across short-horizon and long-horizon tasks. We consider four levels of short-horizon generalization: random placement, crosspart, cross-instance, and cross-category. These generalization primitives are further composed with rigid-object manipulation tasks to form challenging long-horizon activities. Such activities require articulation-aware interaction across multiple generalization axes, as well as reliable language-conditioned task decomposition and sequential execution. An overview is shown in Fig. 1.

Benchmark Scope and Coverage. ArtiBench unifies artic-



Figure 2. Representative tasks from the four ArtiBench scenarios. Examples include disposing trash and organizing items in *Storage*, opening a refrigerator or oven in the *Kitchen*, manipulating drawers and laptops in the *Office*, and placing tools in the *Tool* setting. These tasks illustrate the diversity of everyday articulated interactions.

ulated and rigid-object tasks across four scenarios: Kitchen, Storage, Office, and Tool. It includes diverse articulated categories such as drawers, refrigerators, ovens, toilets, and laptops, along with common storage and office items. All assets are derived from PartNet-Mobility [48], RL-Bench [23], and YCB [7], and all tasks are implemented in CoppeliaSim via PyRep to ensure consistent dynamics and reproducible demonstrations. Our benchmark comprises 98 short-horizon and 34 long-horizon tasks with 449 articulation-related variations, providing a comprehensive evaluation of prismatic and revolute motion patterns across realistic household and office scenarios. Its compact subset, ArtiBench-S, offers a standardized lightweight version that maintains the full evaluation protocol while focusing on the most common articulated-object operations. Representative tasks from the four scenarios are illustrated in Fig. 2.

Generalization Axes. Tasks are structured along five axes that characterize progressive generalization challenges.

- **(L0) Novel Placements** (PL): Tasks involve the same objects and actions as in training but under new spatial configurations, varying initial poses, positions, or distractor arrangements to assess robustness to scene perturbations.
- **(L1) Novel Parts** (PA): The robot must manipulate different articulated parts of a known instance, such as opening the upper, middle, or lower drawer of the same cabinet, thereby evaluating part-level affordance transfer.

Table 1. Comparison of benchmarks for vision-and-language robotic manipulation. For *Train*, *Test* (*short*) and *Test* (*long*), number outside the parentheses is the count of articulation-related tasks and the numbers in parentheses denote the count of articulation-related task variations included in training and evaluation. *Multi*: multiple action primitives; *Transfer*: unseen action—object combinations; *Atc-Task*: articulation-related test tasks; *Atc-Var*: articulation-related test task variations; (PL) / (PA) / (D) / (C): generalization to unseen placements/ articulated parts / instances / categories; (D): long-horizon task compositions.

Benchmark	Simulator	Train	Test (short)	Test (long)	Multi	Transfer	Atc-Task	Atc-Var	Generalization
RLBench-74 [23]	RLBench	1 (1)	19(23)	1(1)	✓	×	20	24	(PL)
VLMBench [55]	RLBench	3 (7)	2 (4)	0 (0)	1	×	5	11	(PL)(I)
Calvin [34]	PyBullet	2 (8)	2 (2)	2(2)	1	×	2	8	(L)
Colosseum [38]	RLBench	3 (5)	3 (5)	1(1)	1	×	4	6	(PL)
GEMBench [15]	RLBench	9 (11)	9 (24)	2 (4)	✓	✓	27	39	PLPAICL
ArtiBench-S (Ours)	RLBench	9 (12)	16 (22)	8 (14)	✓	1	24	36	PL PA I C L
ArtiBench (Ours)	RLBench	28 (31)	98 (300)	34 (149)	✓	✓	132	449	PL PA I C L

Table 2. Short-horizon task coverage (L0-L3) in ArtiBench-S.

Primitive	L0	L1	L2	L3
Open	Drawer top Drawer bottom Drawer2 top Drawer2 bottom	Drawer middle Drawer2 middle	DrawerSmall DrawerLong	-
Open (revolute)	Oven3 Box	-	-	Trashcan Toilet
Close (prismatic)	Drawer top Drawer bottom	Drawer middle	-	-
Close (revolute)	Laptop Lid Microwave Fridge Cabinet2	-	Cabinet5 Microwave2	Toilet

(L2) Novel Instances ①: This level tests generalization across unseen instances within the same category that differ in geometry, scale, or joint limits, for example adapting from a three-drawer cabinet to one with four drawers.

(L3) Novel Categories ©: Tasks require transferring learned manipulation strategies to entirely new articulated categories, for instance generalizing skills learned from laptops to ovens or grills.

(L4) Novel Long-Horizon Tasks ①: The most challenging level involves composing multiple short-horizon primitives from previous levels into temporally extended task sequences. Typical examples include multi-step procedures such as *open_drawer* → *pick/place item*, or *open_oven* → *insert/remove tray*. Short-horizon tasks (L0–L3) in ArtiBench-S are summarized in Tab. 2. Representative long-horizon tasks (L4) from the full ArtiBench are presented in Tab. 3. Comprehensive task lists and configuration details are provided in the supplementary material.

4. ArtiBrain

While existing visuomotor policies excel in short-horizon or single-object settings, they struggle to reason over sequential dependencies and to coordinate different control

Table 3. Representative long-horizon tasks (L4). Each task composes sequential primitives involving both articulated and rigid-object interactions. Comprehensive task configurations and variations are detailed in the supplementary material.

Domain	Task	Sub-task chain	Var.
Storage	bin_dispose_trash	open_bin → pick_trash → place_in_bin	3
Kitchen	oven_place_food	$open_oven \rightarrow pick_food \rightarrow place_in_oven$	8
Office	drawer_store_stationery	open_drawer → pick_stationery → place_in_drawer	12
Tools	toolbox_store_tools	$open_toolbox \rightarrow pick_tool \rightarrow place_in_box$	1

regimes required by rigid and articulated objects. Different from prior modular or monolithic frameworks [13, 42, 54, 57], our ArtiBrain has a novel hierarchical architecture, that unifies open-vocabulary reasoning, hybrid control, and adaptive affordance transfer within a closed-loop pipeline.

At each timestep t, our agent receives multi-view RGB-D images I_t , point clouds P_t , and proprioceptive states S_t . The objective is to learn a policy $\pi(a_t \mid O_t, l)$, where $O_t = \{I_t, P_t, S_t\}$ and l denotes an open-vocabulary instruction. The action a_t specifies the robot control command, including end-effector motion and gripper actuation. Unlike previous end-to-end visuomotor models that directly regress actions from pixels, ArtiBrain explicitly decomposes decision-making into reasoning, control, and memory components, enabling interpretable, generalizable, and self-correcting behavior in long-horizon articulated manipulation.

Our ArtiBrain consists of three modules: (i) VLM-based Task Reasoner. A vision—language model serves as an embodied semantic planner that parses open-vocabulary instructions into structured sub-tasks with success conditions, predicts manipulation type, and issues real-time verification for adaptive replanning or retrying, enabling grounded and interpretable task reasoning. (ii) Hybrid Controller. A novel dual-branch controller dynamically selects between a geometry-guided keyframe policy (GeoKeyframe) for structured rigid-object motions and an affordance-guided diffusion policy (ArtiDiffusion) for

contact-rich articulated interactions, achieving both efficiency and generalization. (iii) Affordance Memory Bank. A self-expanding memory accumulates verified part-level affordances from successful interactions, enhancing transfer across parts and categories.

4.1. VLM-based Task Reasoner

Unlike conventional perception modules that passively interpret visual input, the VLM in our ArtiBrain is designed as an *embodied semantic reasoning agent* that bridges natural-language intent and executable robot control. Before execution, it analyzes the current scene to decompose the instruction into semantic sub-tasks and select the most informative observation view from multi-view inputs to guide downstream controllers. Given the natural-language instruction l and initial observation I_0 , the VLM produces a structured plan Π :

$$\Pi = [(p_i, o_i, c_i)]_{i=1}^N, \tag{1}$$

where Π denotes an ordered sequence of N sub-tasks, p_i represents a primitive action type, such as *open* or *pick*, o_i specifies the semantically grounded target object, and c_i denotes the corresponding success condition.

An overview of this reasoning and execution process is illustrated in Fig. 3. As shown, the VLM decomposes the instruction into actionable sub-tasks, while also generating the corresponding success validation criteria for each task. This structured reasoning enables dynamic adaptation to task complexities and ensures that each action is performed correctly before moving to the next step.

During execution, our controller can select the motion branch for each primitive p_i and performs the action. After each step, the verifier checks whether the success condition c_i is met using visual feedback and task-specific cues such as grasp detection, drawer displacement, or object placement. If c_i is unsatisfied, the controller refines the motion; once satisfied, the system advances to the next subtask, maintaining closed-loop, robust progression. Verified articulated interactions are stored in the Affordance Memory Bank, enabling continual improvement and long-horizon execution.

4.2. Hybrid Controller

To execute each primitive p_i , we employ a novel hybrid controller that selects the motion strategy based on the manipulation mode inferred by the VLM. We formalize the control policy as:

$$a_t = \mathcal{C}_{p_i}(o_i, I_t, D_t, S_t), \qquad \mathcal{C}_{p_i} \in \{\mathcal{C}_{rigid}, \mathcal{C}_{art}\},$$
 (2)

where p_i denotes the VLM-predicted action primitive. o_i is the VLM-inferred target object for the current scene and action primitive. I_t and D_t represent the current RGB-D observations from the camera, from which the corresponding

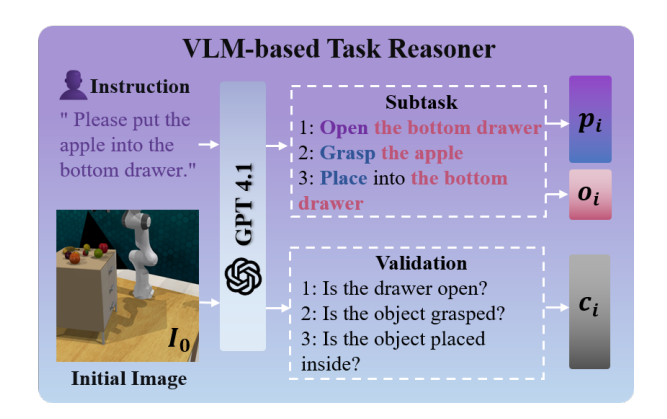


Figure 3. Architecture of our VLM-based Task Reasoner in ArtiBrain. Given a natural-language instruction and initial observation I_0 , the VLM generates a structured plan of sub-tasks (p_i, o_i) with corresponding success conditions c_i . The reasoning process ensures each action is executed and validated before progressing.

point cloud P_t can be derived. S_t denotes the current robot state. An overview of the Hybrid Controller is presented in Fig. 4.

For rigid-object manipulation, our keyframe-based controller $\mathcal{C}_{\text{rigid}}$ (GeoKeyframe) leverages kinematic priors for efficient trajectory planning. For articulated manipulation, we propose a novel part-aware affordance-guided diffusion controller \mathcal{C}_{art} (ArtiDiffusion) that retrieves from the affordance memory to generate continuous actions for contactrich motion planning. These two controllers are dynamically selected by the VLM, enabling robust execution across diverse manipulation scenarios.

4.2.1. GeoKeyframe: Rigid Object Branch

For rigid manipulation actions, we adopt a perception-action pipeline that couples open-vocabulary grounding with 6-DoF grasp synthesis. GPT-4.1 selects the optimal viewpoint from four camera views, and Qwen-VL [3] localizes the target object in the selected image. Multi-Task Masked Transformer (M2T2) [49] operates on the full-scene point cloud and predicts grasp hypotheses across the workspace, each parameterized by an end-effector pose and confidence score. To isolate grasps associated with the grounded target, we back-project the 2D bounding box into 3D and perform KD-Tree nearest-neighbor filtering to retain only grasps whose contact points lie within the target region. Remaining candidates are further pruned through 3D collision checks, yielding a feasible set \mathcal{K} . The final grasp is selected as the highest-confidence feasible prediction:

$$\mathbf{T}^* = \arg\max_{\mathbf{T}_k \in \mathcal{K}} s_k,\tag{3}$$

where s_k denotes the confidence score predicted by the grasp network for candidate T_k . The collision-free trajectory to T^* is then computed and executed by a motion planner using the Open Motion Planning Library (OMPL) [44],

enabling zero-shot grasping of unseen rigid objects.

4.2.2. ArtiDiffusion: Articulated Object Branch

Articulated object manipulation presents a core challenge in robotic control, as it requires accurate contact reasoning and reliable motion planning. To tackle this, we introduce a conditional diffusion policy grounded in retrieved affordance memory, enabling dynamic and contact-aware motion synthesis.

Architecture. The policy comprises four encoders and a U-Net-based denoising network. We extract point cloud features $f_t^P \in \mathbb{R}^{d_P}$ via PointNet [39], encode robot state S_t into $f_t^S \in \mathbb{R}^{d_S}$ via an MLP, and process affordances $\Phi = (c,\tau)$ through two encoders: the contact point c is encoded into $f_c^\Phi \in \mathbb{R}^{d_c}$ via an MLP, while the trajectory sequence τ is encoded into $f_\tau^\Phi \in \mathbb{R}^{d_\tau}$ via a Transformer encoder. These features are concatenated as the global conditioning vector $\mathbf{f}_t = [f_t^P, f_t^S, f_c^\Phi, f_\tau^\Phi]$.

The denoising network ϵ_{θ} is a 1D temporal U-Net that processes the initial noised action sequence $\mathbf{a}_t^k \in \mathbb{R}^{H \times d_a}$. Global conditions \mathbf{f}_t are injected at each layer via Featurewise Linear Modulation (FiLM) [37], which adaptively modulates the intermediate features based on the concatenated context. Combined with sinusoidal embeddings for the diffusion timestep k, the network outputs predicted noise $\epsilon_{\theta}(\mathbf{a}_t^k, k, \mathbf{f}_t)$.

Training and Inference. During training, for each sample in the batch, we randomly sample a diffusion timestep $k \sim \text{Uniform}(1,K)$ and Gaussian noise $\epsilon^k \sim \mathcal{N}(0,I)$. We then minimize the mean squared error (MSE) between the actual noise and the network's prediction:

$$\mathcal{L} = \|\epsilon^k - \epsilon_{\theta}(\mathbf{a}_t^k, k, \mathbf{f}_t)\|^2, \tag{4}$$

where $\mathbf{a}_t^k = \sqrt{\alpha_k} \, \mathbf{a}_0 + \sqrt{1 - \alpha_k} \, \epsilon^k$, is the noised action formed by adding ϵ^k to ground truth \mathbf{a}_0 , and the loss is computed as the MSE averaged over the training batch.

At inference, we apply DDIM [43] sampling for efficient denoising from $\mathbf{a}_t^K \sim \mathcal{N}(0, I)$:

$$\mathbf{a}_{t}^{k-1} = \sqrt{\alpha_{k-1}} \left(\frac{\mathbf{a}_{t}^{k} - \sqrt{1 - \alpha_{k}} \,\hat{\epsilon}_{t}^{k}}{\sqrt{\alpha_{k}}} \right) + \sqrt{1 - \alpha_{k-1}} \,\hat{\epsilon}_{t}^{k},$$
(5)

where $\hat{\epsilon}_t^k = \epsilon_{\theta}(\mathbf{a}_t^k, k, \mathbf{f}_t)$. This deterministic sampling provides fast and stable action generation under affordance-guided conditioning.

Affordance Memory Bank. Inspired by AffordDP [47], We maintain a structured memory that stores successful manipulation experiences:

$$\mathcal{M}_{\kappa} = \left\{ (\mathcal{T}_i, v_i, o_i, \Phi_i, I_{0,i}, P_{0,i}) \right\}_{i=1}^{N_{\kappa}}, \tag{6}$$

where each entry includes the task \mathcal{T}_i , variation identifier v_i , target object o_i , affordance $\Phi_i = (c_i, \tau_i)$ with contact point

 c_i and trajectory τ_i , initial RGB crop $I_{0,i}$, and corresponding point cloud $P_{0,i}$. The memory is divided into buckets \mathcal{M}_{κ} indexed by articulation type $\kappa \in \{\text{revolute}, \text{prismatic}\}$. The bucket size N_{κ} denotes the number of stored demonstrations in \mathcal{M}_{κ} .

At test time, given a query crop I^q , we compute its embedding $z^q = \text{CLIP}(I^q)$ and retrieve the most similar demonstration:

$$(\mathcal{T}^{\star}, v^{\star}, o^{\star}, \Phi^{\star}, I_0^{\star}, P_0^{\star}) = \arg\max_{i \in \mathcal{M}_{\kappa}} \cos(z^{\mathbf{q}}, z_i^0), \quad (7)$$

where cosine similarity measures visual similarity between query z^q and stored appearances z_i^0 .

Unlike the static memory system from AffordDP [47], our memory supports dynamic updates. After each successful task execution, we append the newly generated demonstration $(\mathcal{T}_i, v_i, o_i, \Phi_i, I_{0,i}, P_{0,i})$ to \mathcal{M}_κ . This continual update mechanism enables online adaptation to novel objects and unseen articulation configurations, progressively enriching the Affordance Memory Bank and improving generalization over time.

Part-Aware Affordance Transfer. While existing methods like AffordDP [47] transfer affordances at the object level, our approach advances this paradigm to the part level, enabling fine-grained localization and alignment of functional components such as handles or lids. The retrieved affordance $\Phi^{\rm src}=(c_{\rm 3D}^{\rm src},\tau^{\rm src})$ is transferred to the target scenario through geometric alignment guided by part-level segmentation. Specifically, we first project the source contact point $c_{\rm 3D}^{\rm src}$ onto the image plane. Given the target RGB-D view $(I_{\rm tgt},D_{\rm tgt})$, we use LangSAM [33] to segment finegrained manipulation parts, crop and upsample both source and target masks, and establish pixel-level correspondence via SD-DINOv2 [52] feature matching:

$$c_{\text{2D}}^{\text{tgt}} = \arg\min_{\mathbf{x}_{\text{2D}}^{\text{tgt}} \in \Omega_{\text{part}}} \left\| \hat{f}(c_{\text{2D}}^{\text{src}}) - \hat{f}(\mathbf{x}_{\text{2D}}^{\text{tgt}}) \right\|_{2}, \quad (8)$$

where $\Omega_{\rm part}$ denotes the pixel set within the segmented target part, and $\hat{f}(\cdot)$ is the L2-normalized SD-DINOv2 [52] feature embedding. The matched pixel is then backprojected with depth $D_{\rm tgt}$ to obtain the 3D contact $c_{\rm 3D}^{\rm tgt}$.

For post-contact motion, we use PointSAM [56] to extract part-level point clouds \mathcal{P}_{src} and \mathcal{P}_{tgt} around the contact region, normalize them to local frames, and estimate the rigid transformation $T(\mathbf{x}) = R\mathbf{x} + \mathbf{t}$ via RANSAC-initialized ICP [8, 14]:

$$\min_{R \in SO(3), \mathbf{t}} \sum_{i=1}^{N} \|\mathbf{q}_{i} - (R\mathbf{p}_{i} + \mathbf{t})\|_{2}^{2},$$
 (9)

where $\mathbf{p}_i \in \mathcal{P}_{src}$ and $\mathbf{q}_i \in \mathcal{P}_{tgt}$ denote the corresponding 3D points in the source and target parts, respectively.

The trajectory is transformed accordingly, then adjusted by the local contact displacement $\delta = c_{\rm local}^{\rm tgt} - T(c_{\rm local}^{\rm src})$, and denormalized to obtain $\tau^{\rm tgt}$.

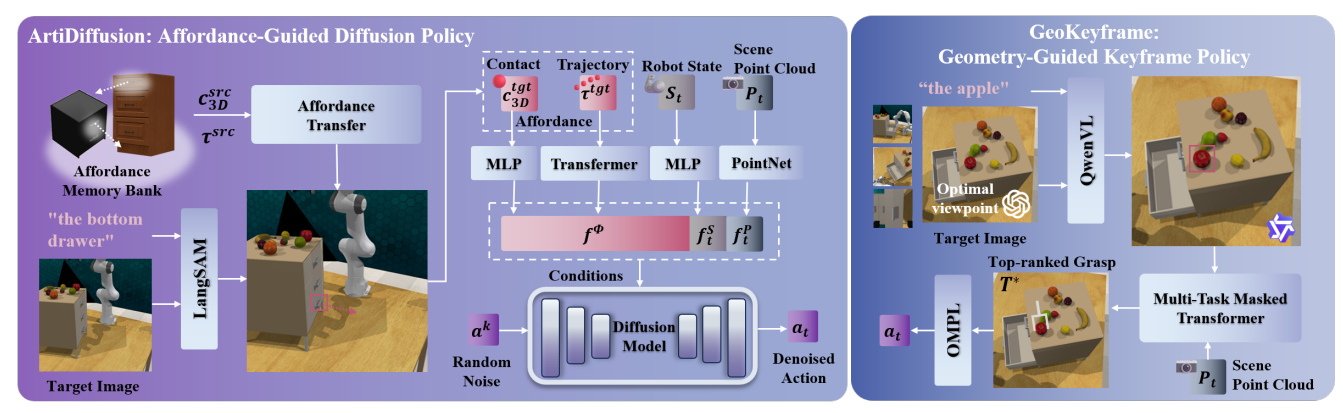


Figure 4. Architecture of the Hybrid Controller in our ArtiBrain. The controller integrates two branches: ArtiDiffusion for articulated object manipulation, employing a four-encoder architecture to extract point cloud features from P_t , encode robot state S_t , and process transferred affordance $\Phi^{\text{tgt}} = (c_{3D}^{\text{tgt}}, \tau^{\text{tgt}})$ obtained by geometrically aligning retrieved source affordance $\Phi^{\text{src}} = (c_{3D}^{\text{src}}, \tau^{\text{src}})$. The fused features condition a diffusion policy that generates action \mathbf{a}_t through temporal U-Net denoising of noised sequence \mathbf{a}^k ; GeoKeyframe for rigid objects, selecting optimal grasp pose \mathbf{T}^* and generating action \mathbf{a}_t via geometric planning.

By incorporating LangSAM [33]-based part segmentation and local geometric registration, our method transfers affordance knowledge at the part level. Our design enables the robot to generalize manipulation strategies across distinct parts and objects with shared articulation semantics, surpassing the generalization capability of object-level frameworks such as AffordDP [47].

5. Experiments

We evaluate our ArtiBrain across two settings: (i) simulation experiments on our ArtiBench, covering progressively harder generalization over *placements*, *parts*, *instances*, and *categories*, as well as *long-horizon* compositional tasks; and (ii) Real-world experiments on a Franka Research 3 (FR3) robot, validating physical transfer and robustness in real environments. All experiments are conducted on a single NVIDIA A40 GPU (48 GB) and the primary evaluation metric is Success Rate (SR, †), defined as the percentage of tasks successfully completed.

5.1. Simulation Results

Baselines. We compare ArtiBrain with three representative state-of-the-art generalization methods: 3D-LOTUS [15], 3D-LOTUS++ [15], and AffordDP [47]. 3D-LOTUS and 3D-LOTUS++ [15] show strong generalization on GEM-Bench [15]. AffordDP [47] generalizes across instances and categories through diffusion. All baselines use official implementations when available and are trained on ArtiBench under identical splits and evaluation settings.

Evaluation Protocol. Each task in ArtiBench is trained with 50 demonstrations and evaluated across the L0–L4 generalization levels, with results averaged over three random seeds.

Results on ArtiBench. As shown in Fig. 5, our ArtiBrain delivers strong performance across all evaluation levels. It

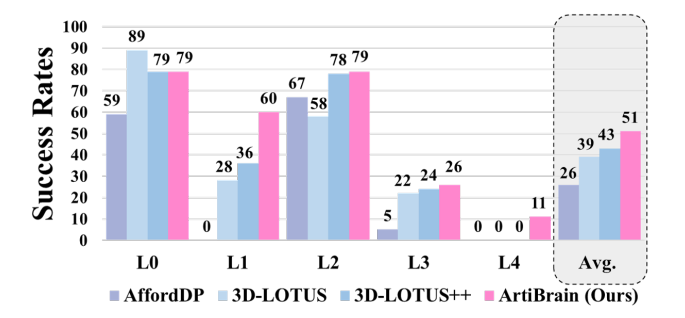


Figure 5. Results on ArtiBench. All numbers denote success rates (%), averaged over three random seeds. ArtiBrain achieves the best generalization performance across L1–L4 levels.

achieves a 60.0% success rate on novel-part tasks (L1), outperforming the strongest baseline by 67%. Moreover, it achieves the strongest performance on long-horizon compositional tasks (L4) and is the only method that successfully completes these tasks. ArtiBrain also achieves strong instance-level (L2) and category-level (L3) generalization, outperforming 3D-LOTUS and 3D-LOTUS++ [15] on both levels and contributing to the highest overall average success rate among all compared methods. These results indicate that our part-aware affordance transfer mechanism enables robust performance under significant geometric, articulation, and temporal variation. Additionally, our ArtiBrain can directly transfer manipulation knowledge learned from short-horizon skills to long-horizon articulated tasks without training needed.

While 3D-LOTUS and 3D-LOTUS++ [15] perform well on near-distribution tasks, their language-conditioned point-cloud policies are trained via behavior cloning on low-level gripper actions and therefore lack explicit mechanisms for articulated part selection or geometry-aware adaptation. Consequently, their performance drops markedly on







(b) Long-horizon task performance.

Figure 6. Real-world setup and long-horizon task performance. (a) Experimental setup with the FR3 robot and D455 RGB-D camera. (b) Example long-horizon scenarios combining articulated and rigid interactions, such as placing household items into drawers and cabinets.

L1–L3 when object geometry or articulation varies. Although 3D-LOTUS++ [15] incorporates LLM-based planning and VLM-based grounding, its controller remains stepwise and open-loop, limiting its ability to maintain temporal consistency in multi-step articulated interactions. In contrast, ArtiBrain integrates part-aware affordance transfer with structured, closed-loop multi-step execution, achieving substantially stronger performance across L1–L4.

5.2. Real-World Results

We evaluate ArtiBrain in real-world articulated manipulation using a FR3 robot with an Intel RealSense D455 RGB-D camera providing front-view observations. The setup includes four articulated and nineteen rigid objects with both revolute and prismatic joints, as shown in Fig. 6(a). Rigid-object pick-and-place operations are planned using the MoveIt! [10] framework to reach target poses predicted by the policy. The evaluation covers two representative articulated tasks, *OpenDoor* and *PullDrawer*, along with long-horizon compositions that combine articulated and rigid-object interactions.

As illustrated in Fig. 6(b), ArtiBrain performs reliably in long-horizon settings, consistently executing opening and pulling motions and completing extended tasks that involve placing household items into drawers and cabinets. These results demonstrate that our ArtiBrain transfers manipulation strategies learned from limited joint-level demonstrations to unseen articulated objects and multi-step scenarios, achieving robust generalization in real-world conditions.

5.3. Ablation Studies

Tab. 4 reports results on representative articulated tasks across all L1–L4 levels. Removing the VLM-based Task Reasoner causes a significant performance drop, particularly in long-horizon L4 tasks, as the model fails to decom-

Table 4. Ablation study on ArtiBench. VLM-based Task Reasoner includes task parsing, sub-goal decomposition, and success verification; LangSAM denotes the language-guided segmentation module.

VLM-based Task Reasoner	LangSAM	L1	L2	L3	L4
✓	✓	40.7	48.4	40.0 40.0 11.0	12.8
_	✓	28.0	40.8	40.0	0.0
_	_	0.0	24.3	11.0	0.0

pose high-level instructions into coherent subgoals and to maintain temporal consistency. Disabling LangSAM [33] primarily reduces part- and instance-level generalization across L1–L3, as the model struggles to distinguish semantically similar components such as multiple drawers or cabinet doors in one scene, leading to inaccurate contact point localization. The variant without both modules performs worst across all levels, confirming that the reasoning module provides goal-directed task decomposition and temporal consistency, while LangSAM [33] ensures spatial grounding and affordance alignment. Their integration enables robust and geometry-aware reasoning for articulated manipulation.

6. Conclusion

In this work, we introduced ArtiBench, a structured benchmark for evaluating generalization in articulated manipulation across four scenarios and five levels of difficulty. Building on this testbed, we proposed ArtiBrain, a unified framework that couples a VLM-based Task Reasoner with a Hybrid Controller for both rigid and articulated object manipulation. Experiments on ArtiBench show that our ArtiBrain achieves state-of-the-art performance in partlevel transfer and long-horizon tasks. Remaining challenges

include VLM hallucination and robust affordance transfer, which we aim to address in future work.

References

- [1] Bo Ai, Stephen Tian, Haochen Shi, Yixuan Wang, Tobias Pfaff, Cheston Tan, Henrik I. Christensen, Hao Su, Jiajun Wu, and Yunzhu Li. A review of learning-based dynamics models for robotic manipulation. *Science Robotics*, 2025. 2
- [2] Baris Akgun, Maya Cakmak, Karl Jiang, and Andrea L Thomaz. Keyframe-based learning from demonstration: Method and evaluation. *International Journal of Social Robotics*, 2012. 2
- [3] Jinze Bai, Shuai Bai, Shusheng Yang, Shijie Wang, Sinan Tan, Peng Wang, Junyang Lin, Chang Zhou, and Jingren Zhou. Qwen-VL: A Frontier Large Vision-Language Model with Versatile Abilities. *arXiv preprint arXiv:2308.12966*, 2023. 5
- [4] Suneel Belkhale, Tianli Ding, Ted Xiao, Pierre Sermanet, Quon Vuong, Jonathan Tompson, Yevgen Chebotar, Debidatta Dwibedi, and Dorsa Sadigh. Rt-h: Action hierarchies using language. arXiv preprint arXiv:2403.01823, 2024. 2
- [5] Konstantinos Bousmalis, Giulia Vezzani, Dushyant Rao, Coline Manon Devin, Alex X. Lee, Maria Bauza Villalonga, Todor Davchev, Yuxiang Zhou, Agrim Gupta, Akhil Raju, and et al. RoboCat: A Self-Improving Generalist Agent for Robotic Manipulation. *Transactions on Machine Learning Research*, 2024. 2
- [6] Anthony Brohan, Yevgen Chebotar, Chelsea Finn, Karol Hausman, Alexander Herzog, Daniel Ho, Julian Ibarz, Alex Irpan, Eric Jang, Ryan Julian, and et al. Do as i can, not as i say: Grounding language in robotic affordances. In *Confer*ence on Robot Learning, 2023. 2
- [7] Berk Calli, Aaron Walsman, Arjun Singh, Siddhartha Srinivasa, Pieter Abbeel, and Aaron M. Dollar. Benchmarking in Manipulation Research: Using the Yale-CMU-Berkeley Object and Model Set. *IEEE Robotics & Automation Magazine*, 2015. 3
- [8] Yang Chen and Gérard Medioni. Object modelling by registration of multiple range images. *Image and Vision Computing*, 1992. 6
- [9] Cheng Chi, Siyuan Feng, Yilun Du, Zhenjia Xu, Eric Cousineau, Benjamin C. M. Burchfiel, and Shuran Song. Diffusion Policy: Visuomotor Policy Learning via Action Diffusion. In *Proceedings of Robotics: Science and Systems*, 2023. 2, 3
- [10] David Coleman, Ioan Sucan, Sachin Chitta, and Nikolaus Correll. Reducing the barrier to entry of complex robotic software: A moveit! case study. arXiv preprint arXiv:1404.3785, 2014. 8
- [11] Embodiment Collaboration, Abby O'Neill, Abdul Rehman, Abhinav Gupta, Abhiram Maddukuri, Abhishek Gupta, Abhishek Padalkar, Abraham Lee, Acorn Pooley, Agrim Gupta, and et al. Open x-embodiment: Robotic learning datasets and rt-x models. *arXiv preprint arXiv:2310.08864*, 2025. 2
- [12] Yilun Du, Sherry Yang, Bo Dai, Hanjun Dai, Ofir Nachum, Joshua B. Tenenbaum, Dale Schuurmans, and Pieter Abbeel.

- Learning Universal Policies via Text-Guided Video Generation. In *Advances in Neural Information Processing Systems*, 2023. 2
- [13] Jiafei Duan, Wentao Yuan, Wilbert Pumacay, Yi Ru Wang, Kiana Ehsani, Dieter Fox, and Ranjay Krishna. Manipulate-Anything: Automating Real-World Robots using Vision-Language Models. In Conference on Robot Learning, 2024. 2, 4
- [14] Martin A. Fischler and Robert C. Bolles. Random sample consensus: a paradigm for model fitting with applications to image analysis and automated cartography. *Communications* of the ACM, 1981. 6
- [15] Ricardo Garcia, Shizhe Chen, and Cordelia Schmid. Towards Generalizable Vision-Language Robotic Manipulation: A Benchmark and LLM-guided 3D Policy. arXiv preprint arXiv:2410.01345, 2025. 2, 3, 4, 7, 8
- [16] Ankit Goyal, Arsalan Mousavian, Chris Paxton, Yu-Wei Chao, Brian Okorn, Jia Deng, and Dieter Fox. Ifor: Iterative flow minimization for robotic object rearrangement. In Proceedings of the IEEE/CVF Conference on Computer Vision and Pattern Recognition, 2022. 2
- [17] Jiayuan Gu, Fanbo Xiang, Xuanlin Li, Zhan Ling, Xiqiang Liu, Tongzhou Mu, Yihe Tang, Stone Tao, Xinyue Wei, Yunchao Yao, and et al. ManiSkill2: A Unified Benchmark for Generalizable Manipulation Skills. In *International Conference on Learning Representations*, 2023. 2
- [18] Dingkun Guo, Yuqi Xiang, Shuqi Zhao, Xinghao Zhu, Masayoshi Tomizuka, Mingyu Ding, and Wei Zhan. Phygrasp: Generalizing robotic grasping with physics-informed large multimodal models. arXiv preprint arXiv:2402.16836, 2024.
- [19] Huy Ha, Pete Florence, and Shuran Song. Scaling up and distilling down: Language-guided robot skill acquisition. In *Conference on Robot Learning*, 2023. 3
- [20] Wenlong Huang, Pieter Abbeel, Deepak Pathak, and Igor Mordatch. Language models as zero-shot planners: Extracting actionable knowledge for embodied agents. In *Interna*tional Conference on Machine Learning, 2022. 2
- [21] Wenlong Huang, Chen Wang, Ruohan Zhang, Yunzhu Li, Jiajun Wu, and Li Fei-Fei. VoxPoser: Composable 3D Value Maps for Robotic Manipulation with Language Models. arXiv preprint arXiv:2307.05973, 2023. 2
- [22] Physical Intelligence, Kevin Black, Noah Brown, James Darpinian, Karan Dhabalia, Danny Driess, Adnan Esmail, Michael Equi, Chelsea Finn, Niccolo Fusai, and et al. $\pi_{0.5}$: a vision-language-action model with open-world generalization. *arXiv preprint arXiv:2504.16054*, 2025. 2
- [23] Stephen James, Zicong Ma, David Rovick Arrojo, and Andrew J. Davison. Rlbench: The robot learning benchmark & learning environment. *IEEE Robotics and Automation Letters*, 2020. 2, 3, 4
- [24] Eric Jang, Alex Irpan, Mohi Khansari, Daniel Kappler, Frederik Ebert, Corey Lynch, Sergey Levine, and Chelsea Finn. Bc-z: Zero-shot task generalization with robotic imitation learning. In *Conference on Robot Learning*, 2022. 2
- [25] Yunfan Jiang, Agrim Gupta, Zichen Zhang, Guanzhi Wang, Yongqiang Dou, Yanjun Chen, Li Fei-Fei, Anima Anandku-

- mar, Yuke Zhu, and Linxi Fan. VIMA: General Robot Manipulation with Multimodal Prompts. In *International Conference on Machine Learning*, 2023. 2
- [26] Tsung-Wei Ke, Nikolaos Gkanatsios, and Katerina Fragkiadaki. 3D Diffuser Actor: Policy Diffusion with 3D Scene Representations. arXiv preprint arXiv:2402.10885, 2024. 2, 3
- [27] Alexander Khazatsky, Karl Pertsch, Suraj Nair, Ashwin Balakrishna, Sudeep Dasari, Siddharth Karamcheti, Soroush Nasiriany, Mohan Kumar Srirama, Lawrence Yunliang Chen, Kirsty Ellis, and et al. Droid: A large-scale in-the-wild robot manipulation dataset. arXiv preprint arXiv:2403.12945, 2025. 2
- [28] Eric Kolve, Roozbeh Mottaghi, Winson Han, Eli VanderBilt, Luca Weihs, Alvaro Herrasti, Matt Deitke, Kiana Ehsani, Daniel Gordon, Yuke Zhu, and et al. AI2-THOR: An Interactive 3D Environment for Visual AI. arXiv preprint arXiv:1712.05474, 2022. 3
- [29] Chengshu Li, Fei Xia, Roberto Martín-Martín, Michael Lingelbach, Sanjana Srivastava, Bokui Shen, Kent Vainio, Cem Gokmen, Gokul Dharan, Tanish Jain, Andrey Kurenkov, and et al. iGibson 2.0: Object-Centric Simulation for Robot Learning of Everyday Household Tasks. arXiv preprint arXiv:2108.03272, 2021. 3
- [30] Chengshu Li, Ruohan Zhang, Josiah Wong, Cem Gokmen, Sanjana Srivastava, Roberto Martín-Martín, Chen Wang, Gabrael Levine, Wensi Ai, Benjamin Martinez, and et al. BEHAVIOR-1K: A Human-Centered, Embodied AI Benchmark with 1,000 Everyday Activities and Realistic Simulation. arXiv preprint arXiv:2403.09227, 2024. 2
- [31] Xiaoqi Li, Mingxu Zhang, Yiran Geng, Haoran Geng, Yuxing Long, Yan Shen, Renrui Zhang, Jiaming Liu, and Hao Dong. Manipllm: Embodied multimodal large language model for object-centric robotic manipulation. In Proceedings of the IEEE/CVF Conference on Computer Vision and Pattern Recognition, 2024. 2
- [32] Jacky Liang, Wenlong Huang, Fei Xia, Peng Xu, Karol Hausman, Brian Ichter, Pete Florence, and Andy Zeng. Code as policies: Language model programs for embodied control. arXiv preprint arXiv:2209.07753, 2022. 2
- [33] Luca Medeiros. Language Segment-Anything: SAM with Text Prompt. https://github.com/luca-medeiros/lang-segment-anything, 2024. Accessed: Sep. 14, 2025. 6, 7, 8
- [34] Oier Mees, Lukas Hermann, Erick Rosete-Beas, and Wolfram Burgard. CALVIN: A Benchmark for Language-Conditioned Policy Learning for Long-Horizon Robot Manipulation Tasks. *IEEE Robotics and Automation Letters*, 2022. 2, 3, 4
- [35] Tongzhou Mu, Zhan Ling, Fanbo Xiang, Derek Yang, Xuanlin Li, Stone Tao, Zhiao Huang, Zhiwei Jia, and Hao Su. ManiSkill: Generalizable Manipulation Skill Benchmark with Large-Scale Demonstrations. arXiv preprint arXiv:2107.14483, 2021. 2, 3
- [36] Octo Model Team, Dibya Ghosh, Homer Walke, Karl Pertsch, Kevin Black, Oier Mees, Sudeep Dasari, Joey Hejna, Charles Xu, Jianlan Luo, and et al. Octo: An Open-

- Source Generalist Robot Policy. In *Proceedings of Robotics: Science and Systems*, 2024. 2, 3
- [37] Ethan Perez, Florian Strub, Harm De Vries, Vincent Dumoulin, and Aaron Courville. Film: Visual reasoning with a general conditioning layer. In *Proceedings of the AAAI Conference on Artificial Intelligence*, 2018. 6
- [38] Wilbert Pumacay, Ishika Singh, Jiafei Duan, Ranjay Krishna, Jesse Thomason, and Dieter Fox. THE COLOSSEUM: A Benchmark for Evaluating Generalization for Robotic Manipulation. arXiv preprint arXiv:2402.08191, 2024. 3, 4
- [39] Charles R Qi, Hao Su, Kaichun Mo, and Leonidas J Guibas. Pointnet: Deep learning on point sets for 3d classification and segmentation. arXiv preprint arXiv:1612.00593, 2016.
- [40] Pratyusha Sharma, Antonio Torralba, and Jacob Andreas. Skill induction and planning with latent language. In Proceedings of the 60th Annual Meeting of the Association for Computational Linguistics, pages 1713–1726, 2022. 2
- [41] Lucy Xiaoyang Shi, Brian Ichter, Michael Robert Equi, Liyiming Ke, Karl Pertsch, Quan Vuong, James Tanner, Anna Walling, Haohuan Wang, Niccolo Fusai, and et al. Hi robot: Open-ended instruction following with hierarchical vision-language-action models. In *International Conference on Machine Learning*, 2025. 2
- [42] Mohit Shridhar, Lucas Manuelli, and Dieter Fox. Cliport: What and where pathways for robotic manipulation. In *Conference on Robot Learning*, 2022. 2, 4
- [43] Jiaming Song, Chenlin Meng, and Stefano Ermon. Denoising diffusion implicit models. In *International Conference on Learning Representations*, 2021. 6
- [44] Ioan A. Sucan, Mark Moll, and Lydia E. Kavraki. The Open Motion Planning Library. *IEEE Robotics & Automa*tion Magazine, 2012. 5
- [45] Homer Rich Walke, Kevin Black, Tony Z. Zhao, Quan Vuong, Chongyi Zheng, Philippe Hansen-Estruch, Andre Wang He, Vivek Myers, Moo Jin Kim, Max Du, and et al. BridgeData V2: A Dataset for Robot Learning at Scale. In *Conference on Robot Learning*, 2023. 2
- [46] Rosa Wolf, Yitian Shi, Sheng Liu, and Rania Rayyes. Diffusion Models for Robotic Manipulation: A Survey. Frontiers in Robotics and AI, 2025.
- [47] Shijie Wu, Yihang Zhu, Yunao Huang, Kaizhen Zhu, Jiayuan Gu, Jingyi Yu, Ye Shi, and Jingya Wang. Afforddp: Generalizable diffusion policy with transferable affordance. In Proceedings of the IEEE/CVF Conference on Computer Vision and Pattern Recognition, 2025. 2, 3, 6, 7
- [48] Fanbo Xiang, Yuzhe Qin, Kaichun Mo, Yikuan Xia, Hao Zhu, Fangchen Liu, Minghua Liu, Hanxiao Jiang, Yifu Yuan, He Wang, and et al. Sapien: A simulated part-based interactive environment. In Proceedings of the IEEE/CVF Conference on Computer Vision and Pattern Recognition, 2020. 2, 3
- [49] Wentao Yuan, Adithyavairavan Murali, Arsalan Mousavian, and Dieter Fox. M2T2: Multi-Task Masked Transformer for Object-centric Pick and Place. In *Conference on Robot Learning*, 2023. 2, 5
- [50] Michał Zawalski, William Chen, Karl Pertsch, Oier Mees, Chelsea Finn, and Sergey Levine. Robotic control via

- embodied chain-of-thought reasoning. arXiv preprint arXiv:2407.08693, 2024. 2
- [51] Yanjie Ze, Gu Zhang, Kangning Zhang, Chenyuan Hu, Muhan Wang, and Huazhe Xu. 3D Diffusion Policy: Generalizable Visuomotor Policy Learning via Simple 3D Representations. In *Proceedings of Robotics: Science and Systems*, 2024. 2, 3
- [52] Junyi Zhang, Charles Herrmann, Junhwa Hur, Luisa Polania Cabrera, Varun Jampani, Deqing Sun, and Ming-Hsuan Yang. A tale of two features: Stable diffusion complements dino for zero-shot semantic correspondence. In Advances in Neural Information Processing Systems, 2024. 6
- [53] Wenqi Zhang, Mengna Wang, Gangao Liu, Xu Huixin, Yiwei Jiang, Yongliang Shen, Guiyang Hou, Zhe Zheng, Hang Zhang, Xin Li, and et al. Embodied-reasoner: Synergizing visual search, reasoning, and action for embodied interactive tasks. *arXiv preprint arXiv:2503.21696*, 2025. 2
- [54] Ziyan Zhao, Ke Fan, He-Yang Xu, Ning Qiao, Bo Peng, Wenlong Gao, Dongjiang Li, and Hui Shen. AnchorDP3: 3D Affordance Guided Sparse Diffusion Policy for Robotic Manipulation. arXiv preprint arXiv:2506.19269, 2025. 2, 3, 4
- [55] Kaizhi Zheng, Xiaotong Chen, Odest Jenkins, and Xin Eric Wang. VLMbench: A compositional benchmark for visionand-language manipulation. In Adavances in Neural Information Processing Systems Datasets and Benchmarks Track, 2022. 3, 4
- [56] Yuchen Zhou, Jiayuan Gu, Tung Yen Chiang, Fanbo Xiang, and Hao Su. Point-SAM: Promptable 3D Segmentation Model for Point Clouds. arXiv preprint arXiv:2406.17741, 2024. 6
- [57] Brianna Zitkovich, Tianhe Yu, Sichun Xu, Peng Xu, Ted Xiao, Fei Xia, Jialin Wu, Paul Wohlhart, Stefan Welker, Ayzaan Wahid, Quan Vuong, and et al. RT-2: Vision-Language-Action Models Transfer Web Knowledge to Robotic Control. In Conference on Robot Learning, 2023.
 2, 4